

# INFLUENCE OF LIGHT ATTENUATION ON BIOFILM PARAMETERS EVALUATED FROM CLSM IMAGE DATA

Anton Semechko<sup>1</sup>, Rangarajan Sudarsan<sup>2</sup>, Elanna Bester<sup>3</sup>, Gideon Wolfaardt<sup>3</sup>, Robert Dony<sup>1</sup>, Michele Oliver<sup>1</sup>, Herman Eberl<sup>2</sup>

<sup>1</sup> School of Engineering, University of Guelph, Guelph, Ontario N1G 2W1, Canada

<sup>2</sup> Department of Mathematics and Statistics and Biophysics, Interdepartmental Program, University of Guelph, Guelph, Ontario N1G 2W1, Canada

<sup>3</sup> Department of Chemistry and Biology, Ryerson University, Toronto, Ontario M5B 2K3, Canada

## 1. INTRODUCTION

Bacterial biofilms are microbial structures growing on surfaces and wetted interfaces in aqueous environments. They form when the bacterial cells attach to the surface and start producing an extracellular polymeric matrix in which the growing bacterial cells embed themselves. Bacterial biofilms play a positive role in waste water treatment while are a hindrance to treatment of bacterial infections in humans. Confocal laser scanning microscopy (CLSM) is the method of choice for studying structure formation of live biofilms in laboratory flow-cell reactors after labeling the bacterial cells with fluorescent markers. Quantitative analysis of the CLSM data, however, requires an accurate segmentation procedure that distinguishes biomass from the surrounding fluid. A literature survey of biofilm segmentation techniques [1] reveals that thresholding [1-5] is the preferred method. This method though simple is not optimal in the presence of noise and depth intensity attenuation (IA) artifacts. Although the former issue was addressed in [5], to our knowledge no attempts have been made by biofilm research community to quantify and remedy the effects of IA in CLSM data of biofilms.

In CLSM images, depth intensity attenuation occurs due to a combination of optical effects which include scattering, absorption and refraction [8-11]. As a consequence, the contrast of images acquired at increasing depth becomes reduced and identification of structures present in the image becomes difficult. Some of the approaches that have been put forth to address this issue are light attenuation modeling [8,9] and histogram renormalization [9,10]. The first approach attempts to restore image quality using physical models of light attenuation which is not practical due to number of simplifying assumptions used. The second approach is based on histogram renormalization techniques which include histogram equalization, dynamic histogram warping (DHW) [9] and histogram specification [10]. According to [10] histogram

equalization and DHW may over-enhance the images, resulting in the appearance of false contours and amplification of noise. Based on these considerations, exact histogram specification can be considered to be a better alternative. In this paper, we implement exact histogram specification as presented in [9] and [10] to perform IA followed by edge enhancing nonlinear diffusion filtering (DF) to suppress noise before performing segmentation using thresholding based on Otsu's method. The importance of doing intensity attenuation correction as a preprocessing step is the primary highlight of this work.

## 2. MATERIALS AND METHODS

Biofilm CLSM image data obtained in [6] of *Pseudomonas* sp. grown in multichannel flow cells with bacteria cells stained with green fluorescent protein was used in our study. The biofilm in [6] was observed using a Zeis CLSM microscope with 20X objective and excitation from 488-nm argon laser. To investigate the effects of intensity attenuation (IA), four biofilm parameters also used in [6] namely biomass, average thickness, roughness and surface to biovolume ratio were chosen. They were evaluated using corresponding routines available in COMSTAT [4] program which runs as a script in Matlab<sup>®</sup>. The definitions of these parameters and the way they are computed is explained in [1] and in COMSTAT user manual [4]. The remainder of this section will describe the image processing procedures that were used to obtain the four biofilm parameters above as well as the validation procedure which was key in demonstrating the effects of IA on biofilm segmentation.

### 2.1 Intensity Attenuation Correction

Depth intensity attenuation is corrected by means of exact histogram specification described in [11,12]. To use this method, the reference histogram,  $H_{ref}$ , must be known beforehand. In [10]  $H_{ref}$  corresponds to the histogram of the "best quality" image in the CLSM

stack. The quality index referred to as automated reference detection estimator (ARDE) (defined as a product of mean intensity, contrast and mean gradient magnitude) is used to make this decision. Higher values of ARDE are expected to correlate with better image quality. The disadvantages of selecting  $H_{ref}$  in this manner is that it may not be representative of the entire data set and consequently lead to over enhancement of images where IA is most pronounced. For this reason  $H_{ref}$  was computed using the standard histogram selection approach described in [9], which was largely based on the work of Nyúl et al. [13]. The main steps of calculating  $H_{ref}$  are described in [9,13].

Once  $H_{ref}$  is known, the intensities of any 2D image can be remapped to produce a histogram which matches  $H_{ref}$  almost exactly. Exact histogram specification is achieved by strict ordering among image pixels as described in [11,12]. The main idea is to refine natural ordering of pixels using the average values of its neighborhood. For every pixel the filter responses are arranged into a feature vector where the first element corresponds to the original intensity value, the second element corresponds to the response of the second filter, etc. These feature vectors are then sorted lexicographically to refine the natural pixel ordering. The overall ordering accuracy (OA) can be measured by the ratio of unique filter responses and the total number of image pixels. For natural images OA is usually above 95% and so induced ordering is very close to being strict.

## 2.2 Nonlinear Diffusion Filtering

Diffusion filtering was used to suppress noise (by encouraging intra-regional smoothing) and enhance the edges of the biofilm structures. Let  $\Omega$  be the image domain and let  $f(\mathbf{x}): \Omega \rightarrow \mathfrak{R}$  be the original image. The filtered image,  $u(\mathbf{x}, t)$ , was obtained as a transient solution of the diffusion equation

$$\partial_t u = \text{div}(D(\nabla u) \cdot \nabla u) \quad (1)$$

with the original image as the initial condition on  $\Omega$ ,  $u(\mathbf{x},0)=f(\mathbf{x})$ , and Neumann boundary conditions equal to zero (which is equivalent to reflecting intensities at the boundaries). In case of an-isotropic diffusion,  $D(\nabla u)$ , is a spatially dependent scalar quantity commonly referred to as diffusivity or an edge-stopping function. Eq.1 was discretized using an explicit scheme described in [14] using 0.1 as a time step value. Due to the size of the volumetric images (1024x1024x23), semi-implicit and implicit schemes were not considered. Diffusivity and contrast threshold parameter intrinsic to it were both computed according to [15].

## 2.3 Segmentation

Once the CLSM images were preprocessed using exact histogram specification and diffusion filtering, biofilm segmentation was performed. The global threshold was calculated using Otsu's criterion designed to maximize the inter-class separability [5] with the biofilm and background making up the two classes. It was observed however, that this approach consistently overestimated the threshold in comparison to the threshold deemed optimal by the operator. This occurrence can be attributed to the unimodal nature of the histogram. To correct for this discrepancy a correction factor was calculated based on the average of manually determined thresholds and applied to the Otsu threshold.

## 2.4 Validation

To demonstrate the effect of depth IA correction on calculation of biofilm parameters steps outlines in Algorithm 1 were performed.

Algorithm 1:

1. In a given CLSM stack, identify the slice which has the highest ARDE score [10]. Let this image be  $I_0$ .
2. Segment  $I_0$  using procedure described in section 2.3 and let this image be  $I_{ref}$ .  $I_{ref}$  is the reference for assessing the accuracy of subsequent segmentation results. To carry out volumetric segmentation assessment  $I_0$  is replicated along z-direction to match the dimensions of the image.
3. Simulate a dataset which has been corrected for depth IA. This is done by specifying  $H_{ref}$  in  $I_0$  and then replicating the resulting image on all levels of the CLSM stack. Call this dataset  $CLSM_{IC}$ .
4. Simulate a dataset which has not been corrected for depth IA. To do this, find the histograms of all cross sections of the CLSM image. Let  $H_i$  be the histogram of the  $i^{th}$  slice. Specify  $H_i$  to  $I_0$  on all levels of the CLSM stack. Call this dataset  $CLSM_{W/O-IC}$ .
5. Perform diffusion filtering as describe in section 2.2 on both  $CLSM_{IC}$  and  $CLSM_{W/O-IC}$ .
6. Segment  $CLSM_{IC}$  and  $CLSM_{W/O-IC}$  as described in section 2.3.
7. Quantify segmentation results from step #6 using  $I_{ref}$  from step #2.

In step #7 segmentation accuracy was quantified using two types of error:

- Err1: Total volume error. This measures the total difference in biofilm volume between  $I_{ref}$  and the segmented image CLSM stack.
- Err2: Average distance from the biofilm surface. This measures the average distance between the surface of  $I_{ref}$  and the surface of the segmented image CLSM stack.

To reduce the bias of the segmentation procedure used to obtain  $I_{ref}$ , the simulated CLSM stacks were partitioned into sixteen equal blocks (of the same height as the CLSM stack). Validation errors were computed for each block and the results from six blocks that had the highest Err1 were discarded. This ensured that only the parts of the CLSM image that were segmented correctly were considered. EMs were then calculated based on the average of the remaining ten blocks.

### 3. RESULTS

The suitability of the proposed biofilm segmentation procedure was tested on 5 sets of CLSM data of *Pseudomonas* sp. biofilm acquired at 24-hour intervals. Each set consisted of 10 CLSM stacks corresponding to different positions along the length of the flow-cell reactor. Figure 1 compares the effects of different preprocessing techniques on four biofilm parameters for CLSM images that were acquired 96 hours after inoculation. To demonstrate the independent and combined effects of IA and DF, biofilm segmentation and subsequent parameter calculations were performed in four different ways: no preprocessing, DF alone, IA alone and IA followed by DF. The four biofilm parameters biomass (P1), average thickness (P2), roughness coefficient (P3) and surface to biovolume ratio (P4) were computed for each case. Figure 2 shows biofilm parameters acquired with the four techniques listed above at five different times. From both Figures 1 and 2 we can conclude that failure to account for intensity attenuation will consistently underestimate P1 and P2 by as much as 50%. It is also interesting to note that there is a very small difference between P1 and P2 extracted from CLSM images without any preprocessing and CLSM images that underwent 20 iterations of the diffusion filter. Furthermore, it appears the value of P3 is least sensitive to the preprocessing methodology and the value of P4 is more dependent on the number of DF iterations than anything else.

Figure 3 shows the validation errors for three types of simulated CLSM data described in section 2.4. Error #1 is the total volume error and Error #2 is average distance from the surface error. The results of P1 and P2 as shown in Figures 1/2a and 1/2b are consistent with the trend of Error #1 in Figure 3a, which clearly demonstrates that without IA correction the biofilm will be considerably under-segmented. Figures 3b and 3c verify that it is IA which is indeed the major source of segmentation error. In Figure 3 the errors are plotted as a function of cross section in the CLSM stack. Note that beyond a certain depth the severity of IA continually increases and it is in these

bottom cross sections (approximately halfway through the CLSM stack) where under-segmentation occurs.

### 4. DISCUSSION

From the above results it is evident that using global thresholding techniques to segment CLSM images of biofilm in the presence of depth intensity attenuation will produce erroneous results. The effect of intensity attenuation can be corrected or minimized during data acquisition [9] if the gain of the CLSM detector is adjusted to maintain a specified mean intensity value. However, if the data had been collected already with a static gain, IA correction is a vital preprocessing step that aides in accurate evaluation biofilm parameters. It is to be noted, that despite its accepted importance, not much has been done in correcting for IA in biofilm research community. IA correction alone does not suffice to ensure accurate segmentation as noise artifacts get enhanced by the histogram specification procedure. For this reason the diffusion filter must be implemented as a secondary preprocessing operation. It is important to note that the validation procedure used to demonstrate the importance of IA correction (section 2.4) did not take into account the effects of noise which according to [8] becomes more prevalent with the increasing depth of the confocal plane. As a consequence the results shown in Figure 3a are not fully representative of the actual CLSM data. In this plot both validation errors are lower prior to DF than with any number of iterations of the DF. Nevertheless this figure still demonstrates the substantial effects of IA on final biofilm segmentation results.

In conclusion, the necessity of IA correction is determined by the image acquisition protocol. In cases where the details regarding the CLSM settings are unavailable, the presence of a decrease in mean intensity indicates that IA is necessary. This trend can be detected automatically thus enabling future implementation of computationally efficient, fully automated and reliable biofilm segmentation procedures.

### REFERENCES

- [1] Z. Lewadowski and H. Beyenal, *Fundamentals of Biofilm Research*, CRC Press inc. Lewis Publishers, Boca Raton, 2007.
- [2] X. Yang, H. Beyenal, G. Harkin and Z. Lewadowski, "Evaluation of biofilm image thresholding methods," *Water Resources*, vol. 35, pp. 1149-1158, 2001.
- [3] H. Beyenal, Z. Lewadowski and G. Harkin, "Three-dimensional structure quantification," *Journal of Microbiological Methods*, vol. 59, pp. 395-413, 2004.
- [4] A. Heydorn *et al.*, "Quantification of biofilm structures by the novel computer program COMSTAT," *Microbiology*, vol. 146, pp. 2395-2407, 2000.

- [5] J. Yerly, Y. Hu, S.M. Jones and R.J. Martinuzzi, "A two-step procedure for automatic and accurate segmentation of volumetric CLSM biofilm images," *Journal of Microbiological Methods*, vol. 70, pp. 424-433, 2007.
- [6] E. Bester, O. Kroukamp, G.M. Wolfaardt, L. Boonzaier and S.N. Liss, "Metabolic differentiation in biofilms as indicated by carbon dioxide production rates," *Applied and Environmental Microbiology*, vol. 76, pp. 1189-1197, 2010.
- [7] Y. Sun, B. Rajwa, and J.P. Robinson, "Adaptive image-processing technique and effective visualization of confocal microscopy images," *Microscopy Research and Technique*, vol. 64, pp. 156-163, 2004.
- [8] Y.Q. Guan, Y.Y. Cai, Y.T. Lee and M. Opas, "Adaptive correction technique for 3D reconstruction of fluorescence microscopy images," *Microscopy Research and Technique*, vol. 71, pp. 146-157, 2008.
- [9] M.C. Capek, J. Jancek and L. Kubinova, "Methods for compensation of the light attenuation with depth of images captured by a confocal microscope," *Microscopy Research and Technique*, vol.69, pp. 624-635, 2006.
- [10] S.G. Stanciu, G.A. Stanciu and D. Coltuc, "Automated compensation of light attenuation in confocal microscopy by exact histogram specification," *Microscopy Research and Technique*, vol. 73, pp. 165-175, 2009.
- [11] D. Coltuc. and P. Bolon, "Strict ordering on discrete images and applications," *Proceedings of ICIP 99*, vol. 3, pp. 150-153, 1999.
- [12] D. Coltuc, P. Bolon and J-M. Chassery, "Exact histogram specification," *IEEE Transactions on Image Processing*, vol. 15, pp. 1143-1152, 2006.
- [13] L.G. Nyúl, J.K. Udupa and X. Zhang, "New variants of a method of MRI scale standardization," *IEEE Transactions on Medical Imaging*, vol. 19, pp. 143-150, 2000.
- [14] P. Perona and J. Malik, "Scale-space and edge detection using anisotropic diffusion," *IEEE Transaction on Pattern Analysis and Machine Intelligence*, vol. 12, pp. 629-639, 1990.
- [15] J.M. Black and D.H. Marimont, "Robust anisotropic diffusion," *IEEE Transaction on Image Processing*, vol. 7, pp. 421-432, 1998.

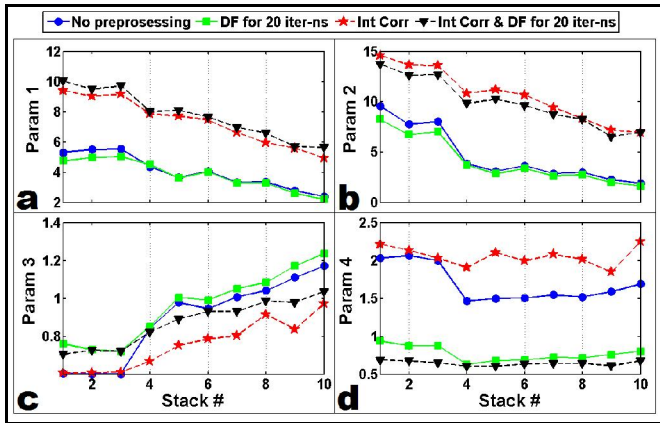


Figure 1: Biofilm parameters shown as a function of position in the flow-cell reactor at 96 hrs after inoculation. (a) Biomass ( $\mu\text{m}^3/\mu\text{m}^2$ ). (b) Average thickness ( $\mu\text{m}$ ). (c) Roughness coefficient. (d) Surface to biovolume ratio ( $\mu\text{m}^2/\mu\text{m}^3$ ).

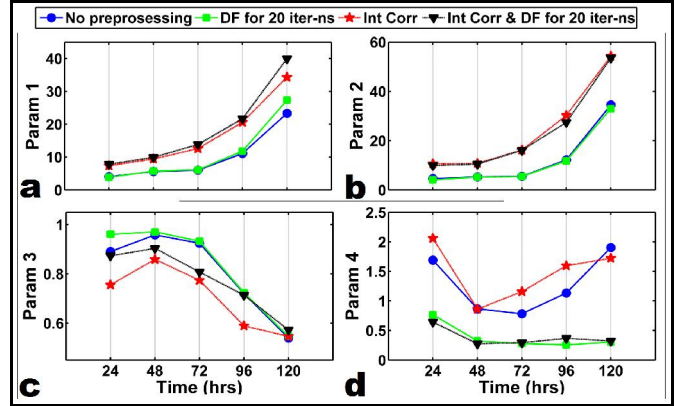


Figure 2: Average biofilm parameters shown as a function of time. (a) Biomass ( $\mu\text{m}^3/\mu\text{m}^2$ ). (b) Average thickness ( $\mu\text{m}$ ). (c) Roughness coefficient. (d) Surface to biovolume ratio ( $\mu\text{m}^2/\mu\text{m}^3$ ).

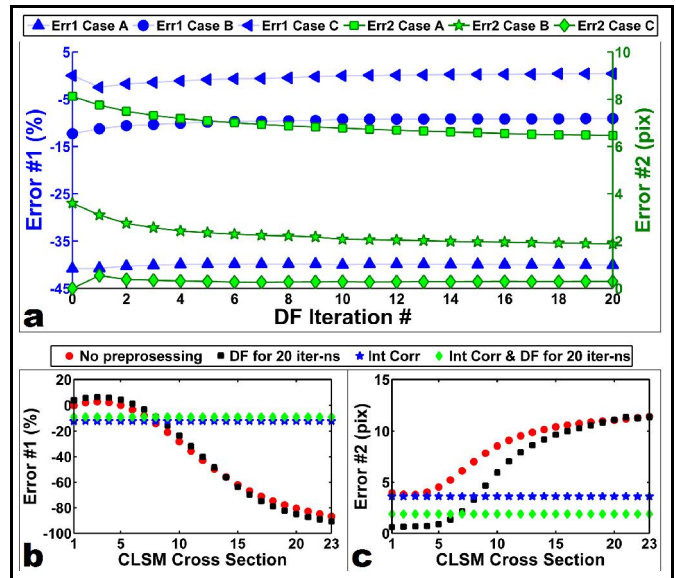


Figure 3: (a) Validation errors for three types of simulated CLSM stacks shown as a function of diffusion filter (DF) iterations (0 corresponds to the initial input to the DF). Case A - no IA correction. Case B - IA corrected using EHS. Case C - unmodified reference image replicated exactly on all levels of the CLSM stack. (b) Biovolume error shown as a function of CLSM cross section for four different preprocessing methods: no preprocessing, DF for 20 iterations, IA correction and IA correction followed by 20 iterations of DF. Negative values indicate that the image is under segmented. (c) Distance from the surface error shown as a function of CLSM cross section.